International Journal of Engineering

Journal Homepage: www.ije.ir

Co-TiO$_2$ Nanoparticles as the Reinforcement for Fe Soft Magnetic Composites with Enhanced Mechanical and Magnetic Properties via Pulse Electrodeposition

M. Vosough, S. Sharafi, G. R. Khayati*

Department of Materials Science and Engineering, Faculty of Engineering, Shahid Bahonar University of Kerman, Kerman, Iran

P A P E R   I N F O

A B S T R A C T

This study is an attempt to produce surface nanocrystalline composite of Fe-Co-TiO$_2$ at various current densities in the range of 20 to 50 mA/cm^2 via pulse electrodeposition method. The prepared composites were characterized by field emission scanning microscope (FESEM), electron dispersive spectrum (EDS), Vickers microhardness, vibrating sample magnetometer (VSM), and x- ray diffraction techniques (XRD). The results showed that the formation of cauliflower morphology was preferred at lower current densities. Moreover, the higher current densities enhanced the Fe content and at the same time diminished the Co and TiO$_2$ contents of prepared surface composites. XRD patterns and Rietveld analysis confirmed the formation of combinations of BCC (as dominant) and FCC phases. Higher current density enhanced the saturation magnetization and decreased lower coercivity due to the higher Fe content and the reduction of TiO$_2$ nanoparticles in coatings. In addition, the lowest coercivity and highest saturation magnetization were gained at 50 mA/cm^2, while, the maximum microhardness obtained at 30 mA/cm^2.

1. INTRODUCTION

Fe-Co alloys are one of the most important structural components due to their amazing magnetism properties [1, 2]. All materials that are magnetized by the application of a magnetic field are called magnetic materials. Depending on how they respond to the magnetic field, magnetic materials are classified as follows:

Ferromagnetic: Some metallic materials have a permanent magnetic moment in the absence of an external field and exhibit very large magnetism and are permanent magnets. Intermediate metals such as iron (in the form of BCC or α-Fe), cobalt and nickel show this property.

Antiferromagnetic: In these materials, the adjacent magnetic moment vectors are equal in the size but in opposite in direction. Therefore, they neutralize each other. If such a material is placed in a magnetic field, the torques are amplified in the same direction as the field, and the material exhibits a weak magnetic property.

Ferrimagnetic: In these materials, the directions of the magnetic moment vectors are adjacent to each other, but their size is not equal. The behavior of these materials is similar to that of ferromagnetic materials.

There is a group of permanent magnets known as ferrites [3]. Films have special properties that are substantially different from their material in bulk. This difference is due to their physical dimensions, geometric shape and microstructure. In addition, these features can be greatly modified to achieve the desired properties [3]. Thin films with thick of submicron and properties caused by their two main features including low thickness and high ratio of surface area with many applications in modern technologies. Some of these features included the increase in resistivity, light interference, tunneling, surface magnetization and critical temperature change of superconductors [4]. According to the performance and properties of the films, they can also be used to improve

*Corresponding Author Institutional Email: *khayatireza@gmail.com*
(G. R. Khayati)

technologies such as solar cells, sensors, optical applications, electronics, and ferroelectrics [4-5].

There are various techniques for the preparation of these alloys including sputtering, sol-gel, molecular beam epitaxy, electrodeposition, and vacuum evaporation [6]. In this regard, low cost, simplicity of electrodeposition, and determination of sediment rate and coating thickness in a wide range caused by the introduction of this process as a hot issue for various areas of research. Significant magnetization (M_s) and negligible coercivity (H_c) are the remarkable characteristics of Fe-Co film produced by electrodeposition. However, these coatings suffer from low mechanical properties, especially hardness; and such disadvantages restricted their usages, significantly [7-8]. In many cases, a ceramic or composite such as metal nanoparticles are utilized to promote the hardness of Fe-Co coatings.

Nevertheless, in the usual mode of direct current electrodeposition, as the procedure continues, one layer of negatively charged type coats the cathode in which is a barrier layer among the deposit-electrolyte interface and charged particles. Pulse electroplating can effectively modify this process [9]. According to the literature, various attempts were carried out to compensate and enhanced the hardness of these coatings by adding oxide nanoparticles or usages of pulse current with respect to the direct current through the preparation of composite coatings [10]. In pulse electrodeposition, the current includes two modes that the layer charges through on-time and discharges somewhat through off-time. This makes swifter transmission of the charged particles via the layer and raises the amount of micro and nano-sized augmentation. In pulse electroplating the duty cycle has been expressed according to Equation (1) [11]:

$$\text{Duty cycle} = \frac{T_{ON}}{T_{ON}+T_{OFF}} = T_{ON}f \tag{1}$$

where T_{ON}, T_{OFF} and f are on-time, off-time and pulse frequency, respectively; frequency has been calculated in the Equation (2):

$$Frequency = \frac{1}{T_{ON}+T_{OFF}} = \frac{1}{T} \tag{2}$$

This research was done to obtain the optimal pulse plating conditions for a cobalt iron coating with titanium dioxide nanoparticles as dopant. The current density has been selected and investigated as the most important factor in current study.

Table 1 summarized the works that have tried to enhance the hardness of these coatings via electrodeposition technique. As abbreviated in Table 1, the main contributions of the current study are:
(i)   Usage of pulse current for preparation of Fe-Co-TiO_2 composite by electroplating;
(ii)   The acceptable saturation magnetization of coatings compared to similar coatings prepared by direct current electrodeposition;
(iii) Usage of relatively negligible reinforcement compared to other researches (about 0.1 vol.%) and as a consequence, its lower relating cost;
(iv)   Determination of residual strength in the prepared coating.

2. EXPERIMENTAL

The chemical materials used in current study were purchased from Merck Company including, iron (III) sulfate (99.99 wt.%), cobalt (II) sulfate (99.99 wt.%), boric acid (99.99 wt.%), L-Ascorbic acid (99.98 wt.%), saccharin and sodium dodecyl sulfate (99.98 wt.%). TiO_2 (99.99 wt.%, 20-30 nm) was provided from US Research Nanomaterials, Inc, USA.

Copper plate (10×10×1 mm) and nickel sheet (20×20×1 mm) were used as cathode and anode,

TABLE 1. Side by side comparison of literatures that compared the mechanical properties of prepared coatings

Ref/year	Coating	Electroplating method		Magnetic parameters		Micro-hardness (HV)	Thickness (μm)	Reinforcement percent (vol.% in bath)	Residual stress (MPa)
		Direct	Pulse	M_s (emu/g)	H_c (Oe)				
Shao/ 2001	Fe-Co-TiO_2	√	-	25.24	150	214.14	20-25	1-2	-
Ghaferi/ 2016	Fe-Co-W	√	-	60-860	76-21	300	18	0.32	-
Iryna Yu/2017	Fe-Co-Mo	-	√	-	-	-	8-10	1.46	-
Yousefi/ 2016	Fe-Ni-TiO_2	-	√	5-16.40	-	536 to 638	-	2.50	-
Takuya Nakanishi/2001	Co-Ni-Fe	-	√	391.79	30<	-	-	-	-
Torabinejad/2017	Fe-Ni-Co	-	√	-	-	519 to 570	120	-	-
Current study	Fe-Co-TiO_2	-	√	13.33-27.83	196.63-122.91	74.3 to 173	20	**0.10**	85 to 253

respectively. The vertical distance of anode to the cathode was adjusted to be about 3 cm. First, the surfaces of cathode copper samples were electro polished at the current density of 1.5 A/m^2 for 60 sec in equi-volume of HNO$_3$ and de-ionized solution to obtain the mirror surface. Afterward, the substrates were washed in acetone and distilled water to eliminate the pollution and then immersed instantly in the electrodeposition cell.

The electrodeposition bath contains, 50 g/L iron (III) sulfate (Fe$_2$(SO$_4$)$_3$), 62.5 g/L cobalt (II) sulfate (CoSO$_4$.7H$_2$O), 30 g/L Boric acid (H$_3$BO$_3$), 3.5 g/L L-Ascorbic acid (C$_6$H$_8$O$_6$), 0.8 g/L saccharin (C$_7$H$_5$NO$_3$S), 0.3 g/L Sodium dodecyl sulfate-SDS (C$_{12}$H$_{25}$NaO$_4$S) and 1 g/L TiO$_2$ nanoparticles. Also, the pulse electroplating parameters for construction of Fe-Co-TiO$_2$ coatings were: current density (20, 30, 40 and 50 mA/cm^2), duty cycle (50 %), pulse frequency (100 Hz), pulse on-off time (5-5 ms), stirring speed (300 rpm), pH (=2) and temperature (25 °C).

The experiments were carried out in plating cell with the volume of 100 mL. Double-distilled water was used as solvent to provide the electrolytes from precursors. pH was controlled by the addition of NaOH and H$_2$SO$_4$. To decrease the possibility of anodic reaction of Fe (ferric to ferrous reaction), use of ascorbic acid as antioxidant was necessary. In addition, sodium dodecyl sulfate as surfactant in the bath was employed to inhibit the agglomeration of TiO$_2$ nanoparticles. All experiments were performed at 25 °C with aggressive stirring rate (300 rpm). To plate each sample and having the films with similar thickness, the electric charge has been kept at 50 coulombs. Rectifier model BHP 2056 used to provide direct current through the electrodeposition. Various current densities in the range of 20-50 mA/cm^2 were applied at constant deposition time equal to 20 min. In addition, the pulse frequency and duty cycle were fixed at permanent fluctuation of 100 Hz and 50 %, respectively. The time of "On" and "Off" were set to 5 msec.

To investigate the surface characteristics, including chemical composition and morphology field emission scanning electron microscopy (FESEM, Hitachi S4160 model) equipped with the EDX point chemical Analyzer were used [8-10]. The phase analyses of Fe-Co-TiO$_2$ films were done by XRD technique (Philips, X'pert-MPD system by Cu-K$_\alpha$). Scherrer equation [12] was used to estimate the average particle size of Fe-Co-TiO$_2$ after the removal of the peak broadening of X-ray due to the instrumental error by Warren's method [12]. Rietveld refinement was performed using materials analysis by diffraction (MAUD) program.

To measure the magnetic properties of the samples VSM (Meghnatis Daghigh Kavir Co. Iran) as magnetic hysteresis loops was used. The samples by dimension of 0.5 mm × 0.5 mm × 1 µm were prepared. Then, the magnetic measurement of samples was performed at 25 °C under the aligned magnetic field to be about ±10000 Oe. Vickers microhardness was used to determine the hardness of the sample by applying the load of 50 g for 15 sec on the sample.

For each sample, evaluation is done on 5 points of the surface and their average was reported as the final valuably. The copper sheet does not have any influence on the microhardness due to the insignificant permeation depth (to be about 1-2 µm) [13].

3. RESULTS AND DISCUSSION

**3. 1. Compositio and Morphology Analysis of Prepared Coatings**   As shown in Figure 1, there is a close relationship between the current density and morphology. Accordingly, it was possible to prepare a dense and smooth Fe-Co-TiO$_2$ coating in the wide range of current densities by adjusting the pulse electrodeposition parameters. During electroplating, the discontinuity of current at certain intervals led to an immense increase in nucleation rate. Hence, the deposited coatings by pulse electroplating have higher density and smaller grain sizes, so that a smoother surface is expected. In addition, it has been observed that TiO$_2$ nanoparticles were distributed at the surface of depositions. Figs. 1 (a-d) illustrate a mixed morphology containing fine nodular and small needles, which confirm the dispersion of phases containing cobalt and iron through the coatings. Similar observations have been reported for morphological investigation of other investigations [14-16]. The analogous and condensed surface may be due to the utilization of pulse electroplating and the distribution of TiO$_2$ nanoparticles through the sample surface [11]. As shown in the Figure 1(a)-(d), by enhancing of current density, the coatings have become coarser with a great nodule and cauliflower morphologies. It seems that higher current density decreased the amount of TiO$_2$ nanoparticles and Co in the coating.

According to the results, by increasing the current density, micro-cracks are appearing on the surface of samples and have been perceived that the surface of depositions becomes coarser with non-uniformity in morphologies.

There are diverse mechanisms to explain this phenomenon, including that the preferred absorption of intermediary species prevents normal co-deposition performance. By increasing the current density, the conditions have been more appropriate for the formation of hydrogen and by consumption of H$^+$ around the cathode, the pH increased locally. This condition significantly promoted the formation of metallic hydroxide [13, 17-18].
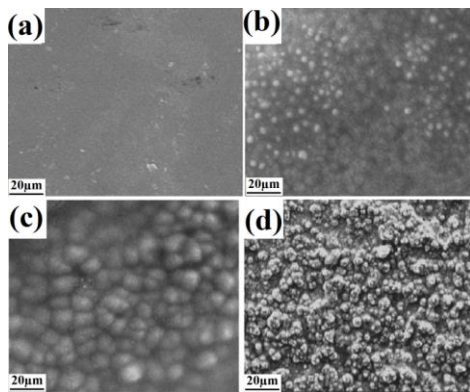
Figure 1. FESEM images of Fe-Co-TiO$_2$ coatings at different current densities prepared at (a) 20, (b) 30, (c) 40 and (d) 50 mA/cm^2
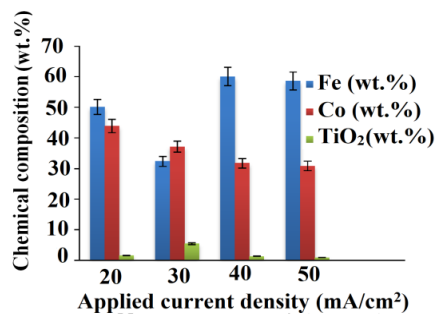
Figure 2. Chemical composition of the coatings at various current densities based on EDX analysis.

Since the desirability to absorb iron hydroxide is higher than that of cobalt hydroxide [19, 20], an increase in the amount of iron deposition is predictable. The white dots in Figure 1 confirm the distribution of TiO$_2$ nanoparticles on the coating which is more clearly seen in Figures 1a and 1b.

Based on the results, it can be concluded that the optimal conditions is satisfied at the current density of 40 mA/cm^2. At this current density, the amount of iron and TiO$_2$ are balanced and a smooth coating with suitable magnetic and mechanical properties is obtained. In addition, the amount of iron on the coating is higher than the prepared coating at 50 mA/cm^2. This is due to anomalous codeposition and less tendency of the noble metal to deposit.

In Figure 1 (current density 30 mA/cm^2), the amount of iron has dropped sharply due to the increase in TiO$_2$ content, so we see larger granules in this current density. The effect of increasing current density on increasing the iron content and reducing the gross amount of coating is confirmed [11, 13, 16]. The mass ratio of the components is determined according to the previous works with different dopants [11, 13]. As illustrated in Figure 2, the weight percent of Co and Fe in the coating for the sample

prepared at 20 mA/cm^2 were 43.9 wt. % and 50.1 wt. %, respectively. However, in the case of 50 mA/cm^2, the weight percent of Co and Fe contents were 30.8 and 58.6 wt. %, respectively. On the other hand, due to the reduction of cathodic over potential, the possibility of a reaction at the electrode surface was decreased. In this condition, the amount of Fe increased in the deposit. According to the literature [21-23], higher current densities enhanced the diffusion of Fe to the coating and as a consequence enhanced the magnetic properties.

As shown in Figure 2, the dependency of current density and TiO$_2$ content in deposition results from two various behaviors. In the range of 20 to 30 mA/cm^2, enhancing the current density increased the TiO$_2$ contents of coatings, while in the range of 40 to 50 mA/cm^2, this behavior was reversed. As shown, the TiO$_2$ content of coating dropped from 5.4 wt. % (in 30 mA/cm^2) to 1.2 wt. % (in 40 mA/cm^2) and 0.8 wt. % (in 50 mA/cm^2). In this regard, by changing the current density from 20 to 30 mA/cm^2, decreasing the rate of iron and cobalt ions has been enhanced due to increasing of metal ions absorbed by TiO$_2$ nanoparticles [24, 25]. By addition of current density (until 50 mA/cm^2) that promotes the deposition speed of metal ions respect to TiO$_2$ particles. This consequence can be related to a greater decrement of metallic ions in electrolyte due to the decreasing rate of metallic ions around the TiO$_2$ is less than the value of it for free metal ions by increasing in current density [11, 26-27].

There are various theories for this phenomenon. According to Lu et al. [4] the preferential absorption of intermediate species prevents normal deposition. As the current density increases, the conditions for hydrogen regeneration become more suitable. In this condition, by consuming H$^+$ around the cathode, the pH in this area will increase and will be the dominant species as hydroxide. Because of the tendency to absorb the iron hydroxide is far greater than that of cobalt hydroxide, the increase in the amount of deposited iron occurs [15, 25].

The prior studies have shown that any increase in the current density up to the critical value extremely enhanced the deposition rate of particles to a maximum value. While, in the current densities than higher than that of this threshold, the possibility of co-deposition of TiO$_2$ nanoparticles was decreased [11]. The behavior of TiO$_2$ nanoparticles explained by Guglielmi's model as a function of current density [11, 13]. Accordingly, the absorption of metallic ions at the surface of nanoparticles had been occurred in the first step. After traveling from the diffusion layer, the surrounded TiO$_2$ nanoparticles with the ionic cover distributed at the cathode. Then, the deposition of TiO$_2$ nanoparticles on the cathode surface takes place weakly. At the same time as the evacuation of metallic ions at the cathode surface occurs, TiO$_2$ nanoparticles accumulated and penetrated inside the Fe-Co coating. Hence, at high current densities including

and over 40 mA/cm^2, the metal deposition process is overcome to the co-deposition of nanoparticles, so it can be seen that in these current densities, significant reduction of nanoparticles inside the coating is visible.

In confirmation of the EDX results, the XRD analysis of samples was also performed. Moreover, in spite of EDX limitations, the usage of this analysis is very common in phase analysis [8-10].

3. 2. Samples Characterization		The structural changes of coatings prepared at various current densities were investigated by XRD patterns (Figure 3). XRD pattern of TiO$_2$ (JCPDS No. 4-0477) confirmed the high purity and crystalline nature of TiO$_2$ nanoparticles as reinforcement. TiO$_2$ peaks with significant intensity were not detected in the XRD patterns of Fe-Co-TiO$_2$ composite coatings. This is due to the very low content (lower than 5 wt.%) of the co-deposited TiO$_2$ nanoparticles in the Fe-Co matrix. Since, in this study TiO$_2$ nanoparticles with anatase phase was used due to its better magnetic properties compared to the other two phases. It was necessary to note that phases less than 5 % by weight cannot be observed in XRD. As shown, there is remarkable dependency between the XRD spectra and relating current density in a way that by an increase in current density, the intensity of cobalt peaks was dramatically diminished. Albeit, there is more Fe, at higher current densities. Similar consequences have been presented by other studies. According to the results, cobalt structures contain two phases , FCC and/or HCP. During electrodeposition, atomic hydrogen may react with cobalt and produce metastable cobalt hydride with FCC structure. Atomic hydrogen is then removed from the sediment due to the decomposition and formation of stable cobalt with HCP structure. It has been reported that the co-deposition of atomic hydrogen with Co in electroplating can create cobalt hydride with low stability and an FCC structure [11]. Dissociation of this phase leads to the removal of hydrogen through the deposition and as a result, Co changes to a more stable HCP phase. Besides this, TiO$_2$ nanoparticles can enhance the performance of preparedness of the structural coating in structural usages. TiO$_2$ peaks with low intensity were observed in XRD spectra of Fe-Co-TiO$_2$ deposited coatings which confirm that very low amount of TiO$_2$ nanoparticles in the Fe-Co coating (maximum of TiO$_2$ was about 5.4 wt. %).

The average grain size of coatings determined by Scherrer equation [12] and the results are summarized in Table 2. Measurements were repeated three times at each angle and the mean values were reported. It can be concluded that the average grain size has been less than 21 nm.

It should be noted that the load transfer process happens in several steps. Transfer ions from electric binary layer to the free positions and their attractions, shallow penetration of adsorbed ions toward the steps, and finally transfer ions from steps to the edges. Any increase in the current density (or higher over potential), enhanced the superficial penetration of ions and the atoms are transmitted faster toward the growing active centers (steps and edges) and consequently facilitated the growth of grains. On the other hand, the germination energy barrier changed by an inverse relationship with the square of over potential. Any increment in the current density increased the over potential. In this condition, the germination rate has enhanced and the grain size will become smaller. It can be concluded that these two parameters compete for the control of the coating grain size. In this research, both factors have similar influences and annihilate their effects. Therefore, the grain size does not show remarkable variations through investigating the region.

Increasing the current density increases the surface penetration of the ions and causes the atoms to move more rapidly to the active growth centers (stairs and edges), thus facilitating the growth of grains. On the other hand, the germination energy barrier is inversely related to the super-potential square. As the current density increases, the germination rate enhances and the grain size becomes smaller. Here, at higher densities, the two factors have the same effect and destroy each other's effects. Therefore, no significant changes in grain size are observed.
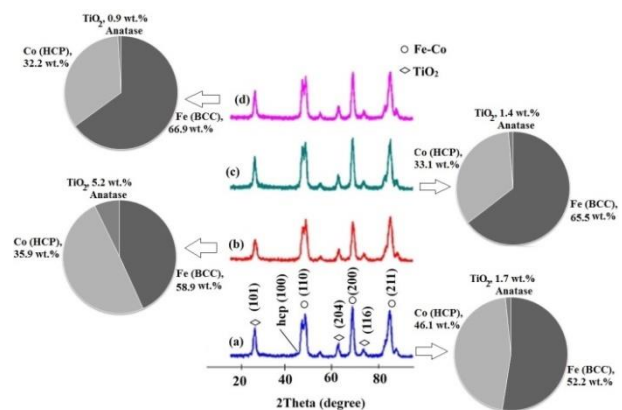
Figure 3. XRD patterns of Fe-Co-TiO$_2$ coatings at different current densities obtained from (a) 20, (b) 30, (c) 40 and (d) 50 mA/cm^2

TABLE 2. Results of Scherrer equation by consideration of various peaks for determination of the average grain size

Current density (mA/cm^2)	2 theta (Degree)	FWHM	Crystallite size (nm)
20	45.25	0.54	15
30	45.70	0.50	19
40	44.68	0.46	21
50	45.10	0.45	21

As shown in Figure 3, the results of Rietveld analysis also confirmed the XRD results and the grain size of the Scherrer equation.

3. 2. Magnetic Properties

Saturation magnetization (M_s) is an inherent characteristic and can be considered as material property. While, coercivity (H_c) is an external characteristics and is a function of several factors such as crystalline nature, chemical composition, particle size, microstructure, thickness, and residual stresses of the prepared coatings by electrodeposition. The hysteresis loops of depositions at various current densities are presented in Figure 4. Moreover, Table 3 shows the magnetic data, i.e., saturation magnetization, for various samples. According to the results, it can be seen that all of the coatings have soft magnetic property (coercivity less than 200 Oe) and any enhancement in the current density, changed the saturation magnetization. Hereon, there is a same opinion, which decrement in non-magnetic element causes for the increase in saturation magnetization. Furthermore, the Fe content of the deposition has an important effect on the saturation magnetization due to the superior magnetic property of iron compared to the other constituents. The most important ferromagnetic elements are cobalt, nickel, and iron, in this sample the higher content of Co can compensate the lower content of Fe in prepared coating [19].

Conforming to the consequences of EDX, the amount of iron in electroplating deposition had increased. However, the TiO_2 content decreased by enhancing the current densities higher than 30 mA/cm^2. Hence, higher current density induced higher saturation magnetization and decreased the coercivity, simultaneously. On the other hand, by an increment in the current density, the amount of TiO_2 nanoparticles decreases, and hence saturation magnetization declines. As mentioned, the coercivity is an extrinsic feature and the grain size is one of the most substantial factors that alter the coercive fields. Decrement in the grain size according to Equation (3) lead to a reduction in magnetic coercivity.

$$H_C = P_c \frac{k_1^4}{J_s A^2} D^6 \tag{3}$$

in which, H_c, A, K_1, J_s, P_c and D, are coercivity, exchange stiffness constant, magneto-crystalline anisotropy, the magnetic moment, a constant of the order of unity and the crystallite size, respectively. By increasing the grain size to the values less than the exchange length, the effect of exchange interactions dominates on the adverse effect of the grain size. Thus, magnetic moments are getting on the same direction, and the coercivity decreases.

For each magnetic material, there is an exchange length, which is explained with Equation (4):

$$L_{ex} = \sqrt{\frac{A}{K_1}} \tag{4}$$

As shown in Equation (5), in the case that the grain size is greater than the exchange length, the coercivity increases due to the reduction in the grain size:

$$H_c \sim \sqrt[3]{\frac{KT_c K_1}{a M_s}} \frac{1}{D} \tag{5}$$

where, M_s, T_c, a, and K are the saturation magnetization, Curie temperature, lattice constant and Boltzmann constant, respectively. It is obvious that the coercivity measurement of iron-based alloys is conforming to the random anisotropy model (RAM). The previous studies demonstrate that the exchange length (L_{ex}) for ferromagnetic material depends on the amount iron in the deposition, so that reduction of iron content leads to the increase in L_{ex}. Consequently, the exchange length was smaller than the grain size for all electroplating coatings (D). Thus, decrementing the grain size led to the increases in coercivity. The results obtained from experimental have a high concordance with RAM theory for all electrodeposition composition. As shown in Figure 5, by enhancing the current density, the coercivity was decreased due to the increase in the grain size. Furthermore, the VSM results revealing the coatings have the soft magnetic property due to the amount of coercivity between 100-200 Oe and thin hysteresis curve. Maximum M_s and minimum of H_c reported in prepared coatings at 50 mA/cm^2 and can be proposed as good candidates for magnetic usages. Also, the amount of reinforcement (TiO_2 nanoparticles) in this sample is at its least, and promotes the magnetic properties due to the presence of higher constituents, i.e., Co and Fe as magnetic elements.

3. 3. Microhardness

The dependency of microhardness and current density are shown in Figure 6. In general, by creating a solid solution, microhardness increases due to the reduction in dislocation mobility. On the other hand, according to Hall-Petch Equation (6), the decrement in the grain size leads to an increase in microhardness:

$$H = H_0 + kD^{-0.5} \tag{6}$$

where H_0 and k are constants related to hardness and D is the grain size obtained by Scherrer equation. Moreover, the consequences display that by increasing the iron content, the microhardness was decreased; so, lower hardness values are related to the greater iron content. In summary, an increase in current density in the range 20-30 mA/cm^2, enhanced the microhardness of coatings. However, in the higher current densities (40 and 50 mA/cm^2), a significant decrement in microhardness has been observed due to the lower content of TiO_2 as reinforcement.

One way to increase the mechanical properties of the coating is to dope ceramic nanoparticles to the composition. The growth of the grains is limited by the
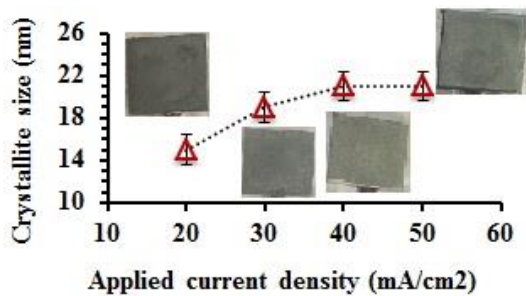
TABLE 3. The saturation magnetization values of Fe-Co-TiO$_2$ coatings as a function of variation of current density (M$_s$ (emu/g))
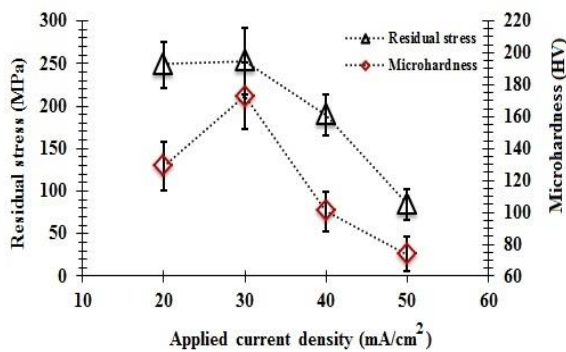
Current density (mA/cm^2)	Saturation magnetization (emu/g)	Coercivity (Oe)
20	13.33	196.63
30	17.61	191.87
40	24.17	146.00
50	27.83	122.91
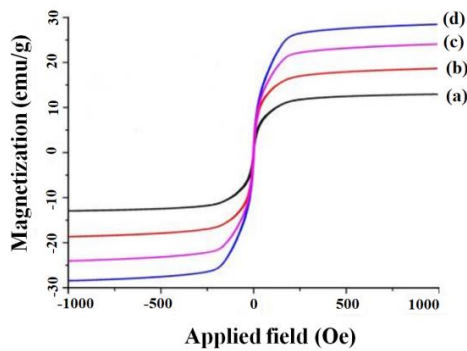
Figure 4. The hysteresis loops of Fe-Co-TiO$_2$ coatings at different current densities (a) 20, (b) 30, (c) 40 and (d) 50 mA/cm^2

Figure 5. The alterations of grain size of coatings at diverse current densities

Figure 6. Effect of current density on the microhardness and residual stress of coatings.

distribution of TiO$_2$ nanoparticles in Fe-Co precipitate. In addition, the plastic deformation process reduces the composition of Fe-Co due to the combined effects of grain refinement and dispersive strengthening mechanisms. The maximum value of microhardness is to be about 173 HV, which is related to 30 mA/cm^2 current density. It means that the amount of TiO$_2$ played an administrated effect on the microhardness.

Residual stress defined as the stresses that remain in a body after the removal of all external forces. This stress can exist as tensile (positive) or compressive (negative). As a general trend, most metal and ceramic coatings have internal stresses. In addition, the compressive stresses in coatings are generally preferred due to the significant improvement of hardness and fatigue life of prepared composites. According to Figure 6, the values obtained from the residual stress and the hardness of the coating is well proportioned. On the other hand, the coatings with higher residual stress have consequently maximum hardness.

As can be seen in Figures 5 and 6, the magnitude of error bars in investigating parameters, i.e., crystalline size, microstructure and residual stress, are proportional to the current densities. In this regard, by increasing the current density to 40 and 50 mA/cm^2, more uniform coverage is obtained and the magnitude of error bars is reduced. In other words, the distribution of data in the range of 40 to 50 mA/cm^2 of current density is more balanced and uniform. This behavior can be related to the higher reproducibility of prepared composites at higher current densities than 40 mA/cm^2.

4. CONCLUSIONS

Preparation of Fe-Co-TiO$_2$ composite using pulse electrodeposition at various current densities is the subject of this study. The structural changes, mechanical and magnetic properties of samples were thoroughly investigated. XRD patterns demonstrated that the dominant structure is BCC. Albeit, increment in the current density led to be added a mixed-phase including BCC and FCC and the saturation magnetization has a direct relationship and coercivity value has a reverse relationship with Fe content of coatings. In addition, by increasing TiO$_2$ nanoparticles, the coercivity value increases. Through the investigated ranges of parameters, the maximum M$_s$, as well as the minimum H$_c$ belonged to the sample at 50 mA/cm^2. Therefore, Fe-Co alloys prepared by pulse electroplating at a current density of 40 mA/cm^2 can be introduced as the optimal coating due to the optimization of magnetic and mechanical properties together. While the maximum amount of residual stress and microhardness belonged to the coatings prepared at 30 mA/cm^2. The other conclusion was the positive effect

of Co in enhanced magnetization saturation at a relatively similar level to the Fe content.

5. REFERENCES

1. Liu, W., Ou, S., Chang, Y., Chen, Y., Liang, Y., Chang, C., Chu, C., Wu, T., "Magnetic properties, adhesive characteristics, and optical properties of Co40Fe40W20 films ", *Surface Engineering*, Vol. 36, (2020), 1-8, DOI: 10.1080/02670844.2020.1753398.

2. Maliar, T., Cesiulis, H., Podlaha, EJ., "Coupled Electrodeposition of Fe–Co–W Alloys: Thin Films and Nanowires", *Frontiers in Chemistry*, Vol. 7, (2019), 542, DOI: 10.3389/fchem.2019.00542.

3. Kołodziej, M., Śniadecki, Z., Musiał, A., Pierunek, N., Ivanisenko, Y., Muszyński, A., Idzikowski, B., "Structural transformations and magnetic properties of plastically deformed FeNi-based alloys synthesized from meteoritic matter", *Journal of Magnetism and Magnetic Materials*, Vol. 502, (2020), 166577, DOI: 10.1016/j.jmmm.2020.166577.

4. Lu, W., Jia, M., Ling, M., Xu, Y., Shi, J., Fang, X., Song, Y., Li, X., "Phase evolution and magnetic properties of FeCo films electrodeposited at different temperatures", *Journal of Alloys and Compounds*, Vol. 637, (2015), 552-556, DOI: 10.1016/j.jallcom.2015.03.036.

5. Toghraei, M., Siadati, H., "Electrodeposited Co-Pi Catalyst on α-Fe2O3 Photoanode for Water-Splitting Applications", *International Journal of Engineering, Transactions C: Aspects*, Vol. 31, No. 12, (2018), 2085-2091, DOI: 10.5829/ije.2018.31.12c.13.

6. Sajjadnejad, M., Omidvar, H., Javanbakht, M., "Influence of pulse operational parameters on electrodeposition, morphology and microstructure of Ni/nanodiamond composite coatings", *International Journal of Electrochemical Science*, Vol. 12, (2017), 3635-3651, DOI: 10.20964/2017.05.52.

7. Pashai, E., Najafpour, G. D., Jahanshahi, M., Rahimnejad, M., "Highly Sensitive Amperometric Sensor Based on Gold Nanoparticles Polyaniline Electrochemically Reduced Graphene Oxide Nanocomposite for Detection of Nitric Oxide", *International Journal of Engineering, Transaction B: Applications*, Vol. 31, No. 2, (2018), 188-195, DOI: 10.5829/ije.2018.31.02b.01.

8. Arjmand, S., Khayati, G., Akbari, G., "Al/Ti5Si3-Al3Ti composite prepared via in-situ surface coating of Ti using tungsten inert gas welding", *Journal of Alloys and Compounds*, Vol. 808, (2019), 151739, DOI: 10.1016/j.jallcom.2019.151739.

9. Sistaninia, M., Doostmohammadi, H., Raiszadeh, R., "Formation Mechanisms and Microstructure Characterization of Al/Al3Ni In-situ Composite by Compound Casting", *Metallurgical and Materials Transactions B*, Vol. 50, (2019), 3020–3026, DOI: 10.1007/s11663-019-01682-1.

10. Adineh, M., Doostmohammadi, H., "Microstructure, mechanical properties and machinability of Cu–Zn–Mg and Cu–Zn–Sb brass alloys", *Materials Science and Technology*, Vol. 35, No. 12, (2019), 1504-1514, DOI: 10.1080/02670836.2019.1630089.

11. Yousefi, E., Sharafi, S., Irannejad, A., "The structural, magnetic, and tribological properties of nanocrystalline Fe-Ni permalloy and Fe-Ni-TiO2 composite coatings produced by pulse electro co-deposition", *Journal of Alloys and Compounds*, Vol. 753, (2018), 308-319, DOI: 10.1016/j.jallcom.2018.04.232.

12. Khayati, G.R., Janghorban, K., "Preparation of nanostructure silver powders by mechanical decomposing and mechanochemical reduction of silver oxide", *Transactions of Nonferrous Metals Society of China*,Vol. 23, (2013), 1520-1524, DOI: 10.1016/S1003-6326(13)62625-4.

13. Ghaferi, Z., Sharafi, S., Bahrololoom, M., "The role of electrolyte pH on phase evolution and magnetic properties of CoFeW codeposited films", *Applied Surface Science*, Vol. 375, (2016), 35-41, DOI: 10.1016/j.apsusc.2016.03.063.

14. Yoosefan, F., Ashrafi, A., Monir vaghefi, S., Constantin, I., "Synthesis of CoCrFeMnNi High Entropy Alloy Thin Films by Pulse Electrodeposition: Part 1: Effect of Pulse Electrodeposition Parameters", *Metals and Materials International*, Vol. 26, (2019), 1262-1269, DOI: 10.1007/s12540-019-00404-1.

15. Barati Darband, Gh., Aliofkhazraei, M., Sabour Rouhaghdam, A., "Facile electrodeposition of ternary Ni-Fe-Co alloy nanostructure as a binder free, cost-effective and durable electrocatalyst for high-performance overall water splitting", *Journal of Colloid and Interface Science*, Vol. 547, (2019), 407-420, DOI: 10.1016/j.jcis.2019.03.098.

16. Saebnoori, E., Vali, I., Yousefpour, M., "Surface Activation of Ni-Ti Alloy by Using Electrochemical Process for Biomimetic Deposition of Hydroxyapatite Coating", *International Journal of Engineering, Transactions A: Basics*, Vol. 27, No. 10, (2014), 1627-1634, DOI: 10.5829/idosi.ije.2014.27.10a.17.

17. Chen, M., Lan, L., Shi, X., Yang, H., Zhang, M., Qiao, J., "The tribological properties of Al0.6CoCrFeNi high-entropy alloy with the σ phase precipitation at elevated temperature ", *Journal of Alloys and Compounds*, Vol. 777, (2019), 180-189, DOI: 10.1016/j.jallcom.2018.10.393.

18. Torabinejad, V., Aliofkhazraei, M., Assareh, S., Allahyarzadeh, M., Rouhaghdam, A.S., "Electrodeposition of Ni-Fe alloys, composites, and nano coatings–A review", *Journal of Alloys and Compounds*, Vol. 691, (2017), 841-859, DOI: 10.1016/j.jallcom.2016.08.329.

19. Khazaei, M., Sarvestani, E., and Khayati, G., "Modeling and optimization of chemical composition of nano/amorphous Fea.Nib.Nbc.Zrd alloy prepared via high-energy ball milling with enhanced soft magnetic properties; A mixture design approach", *Journal of Alloys and Compounds*, Vol. 841, (2020), 155646, DOI: 10.1016/j.jallcom.2020.155646.

20. Lim, D., Ku, B., Seo, D., Lim, C., Oh, E., Shim, S., Baeck, S., "Pulse-reverse electroplating of chromium from Sargent baths: Influence of anodic time on physical and electrochemical properties of electroplated Cr ", *International Journal of Refractory Metals and Hard Materials,* Vol. 89, , (2020), 105213, DOI: 10.1016/j.ijrmhm.2020.105213.

21. Saad, S., Boumerzoug, Z., Helbert, A.L., Brisset, F., Baudin, T., "Effect of TiO2-Nanoparticles on Ni Electrodeposition on Copper Wire", *Metals,* Vol. 10, (2020), 406, DOI: 10.3390/met10030406.

22. Wang, Y., Gao, W., He, Z., Zhang, S., Yin, L., "Improved mechanical properties of Cu–Sn–Zn–TiO2 coatings", *International Journal of Modern Physics B*, Vol. 34, No. 01, (2020), 2040039, DOI: 10.1142/S0217979220400391.

23. Yar-Mukhamedova, G., Ved', M., Yermolenko, I., Sakhnenko, N., Karakurkchi, A., Kemelzhanova, A., "Effect of Electrodeposition Parameters on the Composition and Surface Topography of Nanostructured Coatings by Tungsten with Iron and Cobalt", *Eurasian Chemico-Technological Journal*, Vol. 22, No. 1, (2020), 19-25, DOI: 10.18321/ectj926.

24. Ved', M., Sakhnenko, N., Yermolenko, I., Yar-Mukhamedova, G., Atchibayev, R., "Composition and Corrosion Behavior of Iron-Cobalt-Tungsten", *Eurasian Chemico-Technological Journal*, Vol. 20, No. 2, (2018), 145-152, DOI: 10.18321/ectj697.

25. Seyedraoufi, Z., Mirdamadi, Sh., Rastegari, S., "Electrodeposition of Nano Hydroxyapatite Coating on Biodegradable Mg-Zn Scaffold", *International Journal of Engineering*, Vol. 27, No. 6, (2014), 939-944, DOI: 10.5829/idosi.ije.2014.27.06c.12.

26. Chunyang, M., Danqiong, Z., Zhipeng, M., "Effects of duty cycle and pulse frequency on microstructures and properties of

electrodeposited Ni–Co–SiC nanocoatings", ***Ceramics International***, Vol. 46, (2020), 12128-12137, DOI: 10.1016/j.ceramint.2020.01.258.

27. Yousefi, E., Irannejad, A., Sharafi, S., "Electrodeposition and characterization of nanocrystalline Fe−Ni−Cr alloy coatings synthesized via pulse current method", ***Transactions of Nonferrous Metals Society of China***, Vol. 29, (2019), 2591-2603, DOI: 10.1016/S1003-6326(19)65166-6.

Persian Abstract

چکیده

در این مطالعه سعی شده تا کامپوزیت نانوبلور $Fe-Co-TiO_2$ در چگالی جریان‌های مختلف در بازه ($20-50\ mA/cm^2$) از طریق آبکاری پالسی تهیه شود. کامپوزیت‌های آماده شده با روش های FESEM، EDS، ریزسختی‌سنجی ویکرز، VSM و XRD مشخصه‌یابی شدند. نتایج نشان داد که شکل گیری مورفولوژی گل کلم در چگالی جریان پایین‌تر ارجحیت داشته است. علاوه بر این، چگالی جریان بالاتر باعث افزایش مقدار آهن در ترکیب شده و هم زمان از مقدار Co و TiO_2 پوشش ها کاسته می‌شود. الگوهای XRD و آنالیز ریتولد تشکیل ترکیب BCC (به عنوان فاز غالب) و FCC را تایید کرد. چگالی جریان بالاتر به دلیل وجود آهن بیشتر و نانوذرات TiO_2 کمتر، باعث ایجاد مغناطش اشباع بالاتر و همچنین وادارندگی کمتر شده است. همچنین، کمترین وادارندگی و بیشترین مغناطش اشباع در چگالی جریان $50\ mA/cm^2$ به دست آمد. این در حالی بود که حداکثر میکروسختی در چگالی جریان $30\ mA/cm^2$ ایجاد شده بود.